Partial cross sections and correlation effects in B^{3+}-He collisions

J. P. Hansen
Institute of Physics, University of Bergen, Allégaten 55, N-5007 Bergen, Norway

A. Dubois
Institute of Physics, University of Bergen, Allégaten 55, N-5007 Bergen, Norway
and Department of Chemistry, H. C. Ørsted Institute, University of Copenhagen, DK-2100 Copenhagen, Denmark

S. E. Nielsen
Department of Chemistry, H. C. Ørsted Institute, University of Copenhagen, DK-2100 Copenhagen, Denmark
(Received 15 July 1991)

Total and partial cross sections are calculated for single-electron capture in B^{3+}-He collisions for projectile energies from 1.0 to 500 keV. Results for a one-electron model and a full two-electron treatment of the electronic wave function are compared. Both procedures compare well with experimental data for total cross sections. However, the two-electron model, which incorporates correlation and relaxation effects, compares most favorably, particularly when partial cross sections are considered. The total single-capture cross sections for higher velocities ($v \approx 2-8$ a.u.) decay in average according to a $v^{-7.2}$ behavior, close to the v^{-7} behavior expected from the Bohr-Lindhard model. The discussion focuses on the role of correlation effects during the collision.

PACS number(s): 34.70.+e

I. INTRODUCTION

Studies of electron-transfer processes in heavy-particle collisions where two electrons are active have been widely studied in recent years [1]. It is well known that effects due to electron-electron interaction may play an important role when such processes are considered. At high energies, when the collision can be analyzed by perturbation methods, the contribution to the cross sections from correlation effects may be isolated [2]. At intermediate and low energies, where the collision amplitudes can only be calculated accurately by nonperturbative methods, an isolation is no longer possible. In this case one may obtain understanding of correlation effects by comparing results from one-electron models with full two-electron treatments [3]. In addition, one may study correlation effects by turning the related couplings on or off in the collision program [4].

Total cross sections for single capture in B^{3+}-He collisions have been measured by Zwalley and Cable [5] and by Crandall [6]. The $n=2$ shell gives the dominant contribution to the capture probability for this system, and ratios between the $2s$ and $2p$ cross sections have been measured by Matsumoto *et al.* [7]. The measurements cover the projectile energy range from 0.5 to 50 keV and are in good agreement with calculations using molecular orbitals by Shipsey, Browne, and Olson [8]. The detailed capture dynamics for this system has been investigated with respect to propensity rules for orientation in capture to the $B^{2+}(2p_{\pm 1})$ states. From a simplified coupled-channel model, strong propensity for capture into the $B^{2+}(2p_{-1})$ state was predicted [9]. This was confirmed qualitatively in experiments performed by Roncin *et al.* [10].

A new series of measurements for capture into oriented states, covering a broad range of energies, has been performed [11], and will soon be compared to differential cross sections obtained from calculations. In order to perform such a detailed comparison, we have developed a collision code that employs realistic potentials and corresponding atomic basis functions. This approach will be referred to as a one-electron model, since correlation effects are modeled by a screened electron-core potential. In addition, we have developed a two-electron collision code that employs properly symmetrized two-electron basis functions, and procedures for calculation of matrix elements including the electron-electron interaction.

In this paper we report total and partial cross sections for single capture from $He(1s^2)$ to B^{3+} in the projectile energy range from 1.0 to 500 keV. We particularly focus on two-electron effects, i.e., correlation and relaxation. In the next sections we describe the theoretical procedures, followed by a presentation and discussion of the results. Atomic units will be used unless otherwise stated.

II. THEORETICAL MODELS

In the following we describe two models for calculation of the transition amplitudes. In both models the time-dependent Schrödinger equation is solved in the straight-line-trajectory approximation for the heavy-particle motion, $\mathbf{R}(t)=\mathbf{b}+\mathbf{v}t$. The expansion of the wave function in traveling atomic orbitals centered at the nuclei results in a set of coupled equations for the transition amplitudes, c_j,

$$i\underline{S}(b,v,t)\frac{d}{dt}\mathbf{c}=\underline{M}(b,v,t)\mathbf{c} \ . \tag{1}$$

Here $\underline{S}$ is the overlap matrix that is identical to the unit matrix at $t=\pm\infty$, and $\underline{M}$ is the coupling matrix that contains the integrals over the part of the Hamiltonian that is not diagonalized by the states in question. With appropriate initial conditions, the transition amplitudes can be calculated numerically from Eq. (1), and the probability for electron capture to a state characterized by quantum numbers n_f, l_f is given by

$$p^{\text{cap}}_{n_f,l_f}(b,v)=\sum_{m_f}|c^{\text{cap}}_{n_f,l_f,m_f}(b,v,t=+\infty)|^2 , \tag{2}$$

where m_f runs over final magnetic quantum numbers.

In a one-electron model, the target atom is assumed to be represented by a model potential that gives the correct binding energy of the ground state. At low energies, such a model can be expected to work well, since the transfer probabilities are most sensitive to the Q value $(\varepsilon_{\text{initial}}-\varepsilon_{\text{final}})$ of the reaction [12].

An open question concerns the possible modification of the capture probabilities of the one-electron model due to the presence of two electrons in the initial state. Whether or not the probabilities $p^{\text{cap}}_{n_f,l_f}(b,v)$, should be folded by statistical factors related to binomial distributions of independent-particle models depends strongly on the process in question. By denoting the probabilities for all possible processes in a one-electron model by p^{i} (the electron in the initial state after collision), p^{ion} (ionization channels), p^{exc} (excitation channels), and p^{cap} (capture channels), probability conservation implies

$$1=(p^{i}+p^{\text{ion}}+p^{\text{exc}}+p^{\text{cap}})^2 . \tag{3}$$

For two noninteracting identical particles one thus obtains the total probability for single capture

$$\begin{aligned}P^{\text{cap}}_{n_f,l_f}(b,v)&=2(p^{i}+p^{\text{ion}}+p^{\text{exc}})p^{\text{cap}}_{n_f,l_f}\\&=2(1-p^{\text{cap}})p^{\text{cap}}_{n_f,l_f} .\end{aligned} \tag{4}$$

The commonly used factor of 2 is readily obtained in the perturbation limit when $p^{\text{cap}}\ll 1$. It is important to realize that this procedure implicitly assumes the possibility of two-electron transitions. For collisions where state-selective single-capture channels dominate, this procedure becomes rather doubtful. The cross section to single-capture states in such cases would be underestimated at the cost of large probabilities $(p^{\text{cap}}_{n_f,l_f})^2$ for double capture to nonexisting states.

A drawback for one-electron models is the difficulty of describing relaxation effects. One may try to take this into account by performing statistical foldings based on probabilities for capture from the initial state and probabilities for transition from the relaxed $1s$ state of He^+.

$$P^{\text{cap}}_{n_f,l_f}(b,v)=2(1-p^{\text{tran}})p^{\text{cap}}_{n_f,l_f} , \tag{5}$$

where p^{tran} is the probability for any transfer process from the relaxed $He^+(1s)$ state in a B^{2+}-$He^+(1s)$ collision. For single capture this procedure will again become doubtful at low to intermediate energies, since now the probability p^{tran} will be very small for state-selective processes where the transfer fo the "first" electron is likely. The probability for transfer of the second electron will have a very small reaction window [13] in the impact-parameter range for the first process. As a result, the total probability for single capture in this model may often be larger than unity. For double capture, however, where the probability will be given by $p^{\text{tran}}_{n_f,l_f}p^{\text{cap}}_{n_f,l_f}$, this approach may serve as a useful starting point for probing the capture dynamics [3].

In the following we describe the one- and two-electron models in detail. Based on the preceding discussion, we assume that for the one-electron model all effects by the second electron are represented by a He^+ core potential, and refrain from statistical two-electron modifications. Cross sections will thus be calculated by the usual formula

$$\sigma^{\text{cap}}_{n_f,l_f}(v)=2\pi\int_0^\infty db\, bp^{\text{cap}}_{n_f,l_f}(b,v) , \tag{6}$$

for both models.

A. One-electron model

The Hamiltonian of the one-electron model is defined by

$$H(\mathbf{R}(t),\mathbf{r})=-\frac{\nabla^2}{2}+V^t(r)+V^p(r^p) , \tag{7}$$

where V^t models the He^+ core and V^p models the $B^{3+}(1s^2)$ projectile core. The coordinate $\mathbf{r}^p$ is the electronic space coordinate with respect to the projectile center, i.e., $\mathbf{r}^p=\mathbf{r}-\mathbf{R}$. The potentials are approximated by frozen-core exponential forms. They are explicitly given by

$$V^t(r)=-\frac{1}{r}-e^{-\alpha_t r}\left[\frac{1}{r}+\frac{\alpha_t}{2}\right] , \tag{8a}$$

$$V^p(r^p)=-\frac{3}{r^p}-e^{-\alpha_p r^p}\left[\frac{2}{r^p}+\alpha_p\right] , \tag{8b}$$

where $\alpha_t=3.376\,123$ and $\alpha_p=6.0817$. The target potential is very close to the one first used by Opradolce, Valiron, and McCarroll [14]. The present potentials are created by optimizing the solution of the Schrödinger equation,

$$\left[-\frac{\nabla^2}{2}+V\right]\Phi_{nl}=\varepsilon_{nl}\Phi_{nl} , \tag{9}$$

for the ground-state energy $\varepsilon_{n_0 s}$ with respect to the experimental binding energies. Excited states are then obtained by numerical solutions of Eq. (9), keeping the potentials fixed. The wave functions, obtained from Eq. (9) on a numerical mesh, are fitted to a sum of Slater orbitals. Binding energies obtained from this procedure for excited states are in excellent agreement with experimental energies, cf. Table I. The parameters of the wave-function fits are given in Table II. The scattering state is now expanded:

$$\Psi(\mathbf{R}(t),\mathbf{r})=\sum_{i=1}^{N_t}c_i(t)\Phi^t_i(\mathbf{r})+\sum_{i=N_t+1}^{N_t+N_p}c_i(t)\Phi^p_i(\mathbf{r}^p) , \tag{10}$$

TABLE I. One-electron energies (a.u.) for the $B^{2+}(nl)$ states and the He ground state obtained from numerical solution of the Schrödinger equation, Eq. (9), using the model potentials, Eq. (8), compared to experimental energies.

	State	Energy	Expt. binding energy
B^{2+}	$2s$	−1.3915	−1.394
	$2p$	−1.1751	−1.174
	$3s$	−0.5730	−0.573
	$3p$	−0.5154	−0.515
	$3d$	−0.5005	−0.500
He	$1s$	−0.9029	−0.904

where N_t and N_p are the numbers of target and projectile states. Each projectile state is augmented with electron translational factors $\exp[i\mathbf{v}\cdot\mathbf{r}-(v^2t/2)]$. The wave function of Eq. (10) is inserted into the time-dependent Schrödinger equation and the coupled equations for the expansion coefficients, Eq. (1), are readily obtained.

B. Two-electron model

The Hamiltonian of two electrons, initially bound to the He nucleus and perturbed by the core potential of the B^{3+} ion, is defined by

$$H(\mathbf{R}(t),\mathbf{r}_1,\mathbf{r}_2)=\sum_{i=1,2}\left[-\frac{\nabla_i^2}{2}-\frac{1}{r_i}+V^p(r_i^p)\right]+\frac{1}{|\mathbf{r}_1-\mathbf{r}_2|}\ . \tag{11}$$

The basis functions now become Pauli symmetrized wave functions. Since there are no spin-orbit couplings in the Hamiltonian, only basis functions of positive space symmetry need to be considered. The initial $He(1s^2)$ state is obtained numerically from a Hartree-Fock program, and fitted by two $1s$ orbitals, i.e., $\Psi(r_1,r_2)=\phi_i(r_1)\phi_i(r_2)$, where $\phi_i(r)=2.376\,19e^{-2.3575r}+2.270\,74e^{-1.3884r}$, $\varepsilon_{1s^2}=-2.862$. The final states, expressing the capture of one electron in combination with a relaxation of the other electron to a $He^+(1s)$ state $\phi_0(\mathbf{r})$, are given by

$$\Psi_j^p(\mathbf{r}_1,\mathbf{r}_2)=\frac{1}{\sqrt{(2)}}[\phi_0(\mathbf{r}_1)\Phi_j^p(\mathbf{r}_2^p)+\Phi_j^p(\mathbf{r}_1^p)\phi_0(\mathbf{r}_2)]\ . \tag{12}$$

The single-particle states Φ_j^p are identical to those of Eq. (10), cf. Table II.

A significantly larger number of matrix elements needs to be calculated in a two-electron approach compared to a one-electron model. However, all matrix elements that do not contain the electron-electron repulsion potential can be calculated by standard one-electron methods [15], since they basically become products of one-electron-type matrix elements. The correlation integrals between the initial state and final states are also transformed into standard forms of one-electron-type integrals by a multipole expansion of $|\mathbf{r}_1-\mathbf{r}_2|^{-1}$. Since the function ϕ_0 is an S state, only $L=0$, $M=0$ contributes in the multipole expansion, so the matrix element can be written

$$\int d^3r_1d^3r_2[\phi_i^t(\mathbf{r}_1)\phi_i^t(\mathbf{r}_2)]^*\frac{1}{|\mathbf{r}_1-\mathbf{r}_2|}\Phi_j^p(\mathbf{r}_1-R)\phi_0(\mathbf{r}_2)$$
$$=\int d^3r_1\phi_i^{*t}(\mathbf{r}_1)\Phi_j^p(\mathbf{r}_1^p)f(r_1)\ , \tag{13}$$

where

$$f(r_1)=\sum_i\left[a_i\frac{2}{\alpha_i^3}\frac{1}{r_1}-e^{-\alpha_ir_1}\left[\frac{1}{\alpha_i^2}+\frac{2}{\alpha_i^3r_1}\right]a_i\right]\ .$$

TABLE II. Parameters for the analytical fits to the radial part of the one-electron wave functions, $R_{n,l}(r)=\sum_k c_k r^{\beta_k}e^{\alpha_k r}$.

	State	Coefficients						
B^{2+}	$2s$	c_k	1.815 52	2.750 33	−3.974 93	−6.021 63		
		α_k	−2.815 87	−1.709 45	−2.815 87	−1.709 45		
		β_k	0	0	1	1		
	$2p$	c_k	1.705 94	3.329 28				
		α_k	−3.796 98	−1.548 15				
		β_k	1	1				
	$3s$	c_k	0.985 572	1.377 47	−2.741 36	−3.831 43	1.150 77	−2.608 36
		α_k	−2.203 16	−1.103 75	−2.203 16	−1.103 75	−2.203 16	−1.103 75
		β_k	0	0	1	1	2	2
	$3p$	c_k	0.636 314	1.846 61	−0.335 554	−0.973 792		
		α_k	−1.941 53	−1.022 06	−1.941 53	−1.022 06		
		β_k	1	1	2	2		
	$3d$	c_k	0.424 774					
		α_k	−1.002 12					
		β_k	2					
He	$1s$	c_k	2.266 85	2.299 73				
		α_k	−2.354	−1.3815				
		β_k	0	0				

Here a_i refers to the product of normalization factors of the two $1s$ states $\phi_i^t(\mathbf{r}_2)$ and $\phi_0(\mathbf{r}_2)$, and α_i refers to the sum of exponents of the states.

The matrix elements between the final-capture states can be expressed in terms of the usual perturbation from the target ion M_{ij}^{direct}, terms due to relaxation M_{ij}^{ralax}, and terms due to correlation V as

$$M_{ij}^{pp}=M_{ij}^{\text{direct}}+M_{ij}^{\text{relax}}+V_{ij}^{12}+V_{ij}^{21} . \tag{14}$$

In the first correlation integral V_{ij}^{12}, the translational factors are attached to the same space variable. The correlation interaction is then multipole expanded, resulting in a standard type of one-electron integral,

$$V_{ij}^{12}=\int d^3r_1 \Phi_i^{*p}(\mathbf{r}_1^p)\Phi_j^p(\mathbf{r}_1^p)\left[\frac{1}{r_1}-e^{-4r_1}\left[2+\frac{1}{r_1}\right]\right] . \tag{15}$$

The last type of correlation integral, V_{ij}^{21}, originates from the exchange of the two electrons. This integral is the most complicated, and the numerical evaluation is time consuming, since it cannot be brought to a one-electron type of integral. However, since this integral is quite small compared to the other terms of Eq. (14), we attempt to approximate this term. In a zeroth-order approximation it was simply dropped, and in a peaking approximation it was replaced by the product of two relaxation overlaps:

$$V_{ij}^{21}=\int d^3r_1 d^3r_2[\Phi_i^p(\mathbf{r}_1^p)\phi_0(\mathbf{r}_2)]^*\frac{1}{|\mathbf{r}_1-\mathbf{r}_2|}\Phi_j^p(\mathbf{r}_2^p)\phi_0(\mathbf{r}_1)$$
$$\approx\int d^3r_1\Phi_i^p(\mathbf{r}_1^p)^*\phi_0(\mathbf{r}_1)\int d^3r_2\phi_0(\mathbf{r}_2)^*\Phi_j^p(\mathbf{r}_2^p) . \tag{16}$$

With this simplification we have obtained a two-electron procedure where all matrix elements are calculated by the same procedures as for one-electron calculations. None of these approximations affects Galilean invariance and probability conservation of the coupled equations, Eq. (1). In the next section we discuss results of calculations where both types of approximations are used.

III. RESULTS AND DISCUSSION

The Q values for excited He states are so large that to a good approximation only the ground state of He is included in the expansion. On the projectile center, the complete $n=2$ and 3 shells are included. However, we find that the $n=3$ shell, which represents endoergic channels, is only populated by a few percent at the maximum. Thus the present system is very simple and almost ideal for studies of basic capture mechanisms. No double-transfer or transfer-excitation terms are included, which are well-justified approximations, since, e.g., double-capture cross sections are very small [6].

In Fig. 1 we compare results for total-capture cross sections from the two-electron model with experimental results of Zwalley and Cable [5]. Note that the measurements of Crandall [6] within their uncertainty (about ±20%) are in agreement with [5]. The solid curve refers to a calculation employing the peaking approximation of Eq. (16), and the dashed curve refers to a calculation where the V_{ij}^{21} coupling is neglected. The two calculations give very similar results, and it is clear that this coupling is not too important for total-capture cross sections. The estimated error of the experimental cross sections of [5] was reported to be about ±7% so that both calculations are in excellent agreement with experiments. In the following we shall refer to the two-electron calculation as the calculation that uses the peaking approximation.

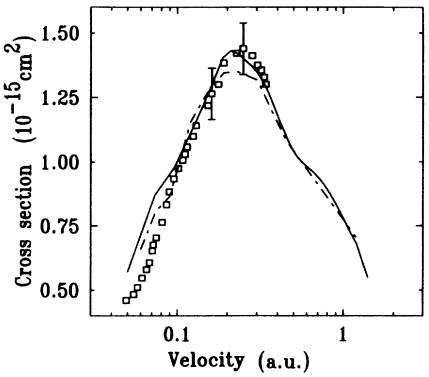

FIG. 1. Total-capture cross sections for the two-electron model compared to the experimental results of Zwalley and Cable [5] (squares). Solid line: calculation using the peaking approximation of Eq. (16). Dashed line: calculation without the term V_{ij}^{21} of Eq. (16).

In Fig. 2 we compare total-capture cross sections for the two-electron model and for the one-electron model. It is clear that the two-electron model gives a better agreement with experiments at the maximum cross section. At low energies, however, the two models tend to the same agreement with experiments, reflecting that the Q value is the most important parameter for such (avoided) curve-crossing reactions. At intermediate energies $v\approx 0.2$, however, correlation and relaxation also play an important role.

It is interesting to compare the behavior of the capture cross sections at higher energies with the simple Bohr-Lindhard model [16]. According to this model, the elec-

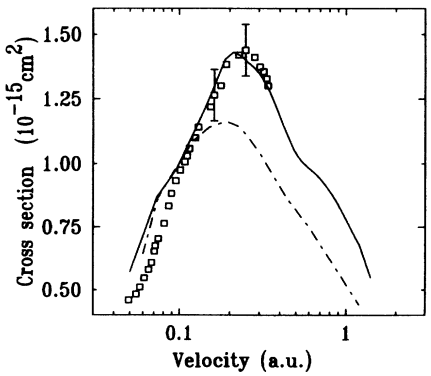

FIG. 2. Total-capture cross sections for the two-electron and one-electron models compared to the experimental results of Zwalley and Cable [5] (squares). Solid line, two-electron model; dashed line, one-electron model.

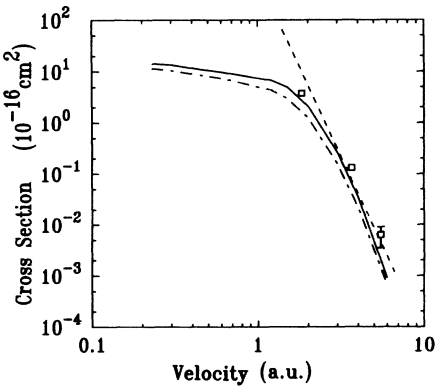

FIG. 3. Total-capture cross sections for the two-electron (solid line) and one-electron (dashed-dotted line) models at higher energies and the prediction of the Bohr-Lindhard model, Eq. (17) (dashed line). Squares are the experimental data of Dmitriev *et al.* [17].

tron must be released from the target at an internuclear separation distance R_r, where the forces felt by the electron from the target and the projectile balance. Then capture may take place at a smaller distance R_c, where the potential energy of the projectile is sufficient to balance the induced translational kinetic energy $\frac{1}{2}v^2$ of the electron. The probability for capture to take place was taken to be the ratio of the collision time R_c/v to the electron orbital time $a_n/v_n \approx 1$, which gives the capture cross section

$$\sigma^{\text{Bohr-Lindhard}} = \pi R_c^2 \frac{R_c}{v} = 8\pi \frac{Z_p^3}{v^7} \quad . \tag{17}$$

Since potential-energy curves and electron translational factors are included in the collision codes, one may expect that the Bohr-Lindhard model compares reasonably well with the calculations at intermediate energies. In Fig. 3 we compare the two models and the result of Eq. 17, and we observe that the behavior is quite similar for $v \approx 2-8$. Both model calculations here show a decay in average according to a $v^{-7.2}$ power law, very close to the Bohr-Lindhard model. Note also the fair agreement of

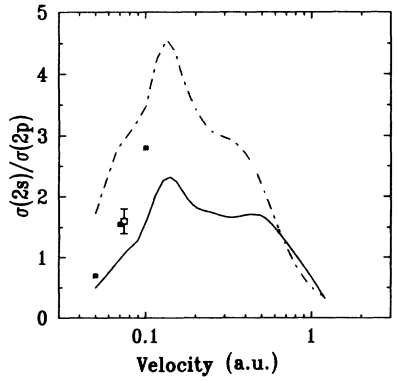

FIG. 4. Ratios of the partial $\sigma(2s)$ and $\sigma(2p)$ cross sections. Solid line, two-electron model; dashed line, one-electron model. Experimental points: Matsumoto *et al.* [7] (closed squares) and Roncin *et al.* [10] (open square).

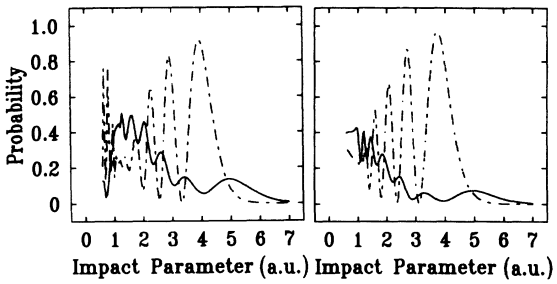

FIG. 5. Probability for capture ($v = 0.2$) to the $2p$ state (solid line) and the $2s$ state (dashed line) for the two-electron (left) and the one-electron (right) models.

our calculations with the experimental results of Dmitriev *et al.* [17].

A more-sensitive test of theoretical models is obtained when comparing partial and differential cross sections. The absolute values of these quantities have not yet been measured, but the fractions σ^{2s}/σ^{2p} have been reported by Matsumoto *et al.* [7] from energy-gain experiments and lately by Roncin *et al.* [10]. We observe in Fig. 4 that the two-electron model slightly underestimates the fraction, but is in better agreement with the data than the one-electron model, which overestimates the fraction. We note the possibility that the discrepancy between the two-electron model and the experiments may be removed by exact evaluation of the correlation integral, cf. Eq. (16).

The origin of the better agreement of the two-electron models can be ascribed to correlation and relaxation effects during the capture process. In fact, if we neglect the correlation coupling of Eq. (13), the total-capture cross section at $v = 0.2$ reduces from 1.42×10^{-15} cm^2 to 1.07×10^{-15} cm^2, which is close to the results of the one-electron model. In Fig. 5 we show the capture probability at this velocity as a function of impact parameter b. We observe that correlation and symmetrization effects give larger contributions to the cross section in the b region from 1 to 3. This contribution can also be identified in differential cross sections. We observe that the "curve-crossing" contribution at $b \approx 5$ becomes slightly larger for the two-electron model.

In conclusion, we have compared results from two-electron and one-electron models of B^{3+}-He($1s^2$) collisions. The two-electron model gives the best agreement with experiments, as expected, but in general both models seem to be applicable in this study of single capture to multiply charged ions. The latter conclusion stands in contrast to the conclusion drawn by Fritsch and Lin [18] from a study of C^{6+}-He collisions, but other mechanisms may play a role for this system. In a future publication [19], the two-electron-model results will be compared to experimental results for differential cross sections for capture into $B^{2+}(2p_{\pm 1})$ states in planar collisions.

ACKNOWLEDGMENTS

A. D. and J. P. H. acknowledge support from the Norwegian Research Council (NAVF), and A. D. and S. E. N acknowledge support from the Danish Natural Science Research Council.

[1] W. Fritsch and C. D. Lin, Phys. Rep. **202**, 1 (1991).
[2] J. H. McGuire, Phys. Rev. A **36**, 1114 (1987).
[3] A. Jain, C. D. Lin, and W. Fritsch, Phys. Rev. A **39**, 1741 (1989).
[4] M. Barat, P. Roncin, L. Guillemot, N. Gaboriaud, and H. Laurent, J. Phys. B **23**, 2811 (1990).
[5] J. H. Zwalley and P. G. Cable, Phys. Rev. A **4**, 2301 (1971).
[6] D. H. Crandall, Phys. Rev. A **16**, 958 (1977).
[7] A. Matsumoto *et al.*, J. Phys. Soc. Jpn. **52**, 3291 (1983).
[8] E. J. Shipsey, J. C. Browne, and R. E. Olson, Phys. Rev. A **15**, 2166 (1977).
[9] J. P. Hansen, L. Kochbach, A. Dubois, and S. E. Nielsen, Phys. Rev. Lett. **64**, 2491 (1990).
[10] P. Roncin, C. Adjouri, M. N. Gaboriaud, L. Guillemot, M. Barat, and N. Andersen, Phys. Rev. Lett. **65**, 3261 (1990).
[11] C. Adjouri and P. Roncin (private communication).
[12] P. Hvelplund, A. Barany, H. Cederquist, and J. O. K. Pedersen, J. Phys. B, **20**, 2515 (1987).
[13] K. Taulbjerg, J. Phys. B **19**, L367 (1986).
[14] L. Opradolce, P. Valiron, amd R. McCarroll, J. Phys. B **16**, 2017 (1983).
[15] J. P. Hansen and A. Dubois, Comput. Phys. Commun. (to be published).
[16] J. S. Briggs, in *Semiclassical Descriptions of Atomic and Nuclear Collisions,* edited by J. Bang and J. de Boer (North-Holland, Amsterdam, 1985); N. Bohr and J. Lindhard, K. Dan. Vidensk. Selsk. Mat. Fys. Medd. **28**, 7 (1954).
[17] I. S. Dimtriev, V. S. Nikolaev, Y. A. Tashaev, and Y. A. Teplova, Zh. Eksp. Teor. Fiz. **67**, 2047 (1974) [Sov. Phys.—JETP **40**, 1017 (1975)].
[18] W. Fritsch and C. D. Lin, J. Phys. B **19**, 2683 (1986).
[19] C. Adjouri *et al.* (unpublished).